JACS
JOURNAL OF THE AMERICAN CHEMICAL SOCIETY

ARTICLE

pubs.acs.org/JACS

Mechanism of Immunoglobulin G4 Fab-arm Exchange

Theo Rispens,* Pleuni Ooijevaar-de Heer, Onno Bende, and Rob C. Aalberse

Sanquin Research, Plesmanlaan 125, 1066 CX, Amsterdam, The Netherlands and Landsteiner Laboratory, Academic Medical Centre, University of Amsterdam, The Netherlands

Supporting Information

ABSTRACT: Immunoglobulin G (IgG) antibodies are symmetrical molecules that may be regarded as covalent dimers of 2 half-molecules, each consisting of a light chain and a heavy chain. Human IgG4 is an unusually dynamic antibody, with half-molecule exchange ("Fab-arm exchange") resulting in asymmetrical, bispecific antibodies with two different antigen binding sites, which contributes to its anti-inflammatory activity. The mechanism of this process is unknown. To elucidate the elementary steps of this intermolecular antibody rearrangement, we developed a quantitative real-time FRET assay to monitor the kinetics of this process. We found that an intrinsic barrier is the relatively slow dissociation of the CH3 domains that noncovalently connect the heavy chains, which becomes rate determining in case disulfide bonds between the heavy chains are reduced or absent. Under redox conditions that mimic the previously estimated in vivo reaction rate, i.e., 1 mM of reduced glutathione, the overall rate is ca. 20 times lower because only a fraction of noncovalent isomers is present (with intra- rather than interheavy chain disulfide bonds), formed in a relatively fast pre-equilibrium from covalent isomers. Interestingly, Fab arms stabilize the covalent isomer: the amount of noncovalent isomers is ca. 3 times higher for Fc fragments of IgG4 (lacking Fab domains) compared to intact IgG4, and the observed rate of exchange is 3 times higher accordingly. Thus, kinetic data obtained from a sensitive and quantitative real-time FRET assay as described here yield accurate data about interdomain interactions such as those between Fab and/or Fc domains. The results imply that in vivo, the reaction is under control of local redox conditions.

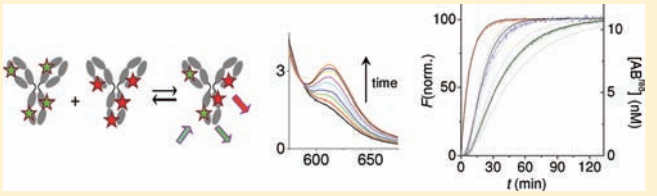

INTRODUCTION

In recent years it has become clear that after secretion, antibodies can undergo structural changes that alter their functionality.[1] The most striking example is human immunoglobulin G4 (IgG4), the least abundant of the four human IgG subclasses. IgG4 becomes effectively monovalent by exchanging half-molecules with other molecules of IgG4, combining random specificities in the second Fab arm for a given specificity of the first Fab arm.[2] Therefore, they cannot cross-link antigen to form immune complexes and thus contribute to the anti-inflammatory activity of IgG4.[3] There are indications that similar processes may take place also in rabbits[4] and mice.[5] It is unknown how this exchange process might be regulated in vivo. Until now, Fab-arm exchange is observed in vitro only in the presence of reducing agents such as reduced glutathione (GSH).

Structurally, the human IgG subclasses are remarkably similar, with an overall >95% sequence identity. This implies that relatively few amino acid differences underlie functional variation between, e.g., IgG1 and IgG4. Compared to IgG1, two structural features of IgG4 are important for the exchange reaction (Figure 1). First, compared to IgG1, the CH3 domain of IgG4 is necessary for exchange to be observed.[2] The (noncovalent) interheavy chain interactions in the CH3 domains are most likely significantly weaker, thereby allowing dissociation, an inevitable step in the exchange process. Second, a serine instead of proline at position 228 in the core hinge further facilitates exchange, probably because the hinge is more easily reduced, since the exchange reaction can be observed at higher concentrations of GSH also if this feature is absent. Introducing both features in IgG1 results in a mutant antibody that is able to exchange half-molecules similar to IgG4.

Whereas the first feature is intuitively clear, i.e., weaker interactions between heavy chains facilitating dissociation, the role of the hinge region is less obvious. In both IgG1 and IgG4, the core hinge is formed by a CXXC motif (Figure 1), also found in redox-reactive proteins such as thioredoxins.[6] In IgG1 the motif is CPPC, and although in principle an intrachain disulfide bond may form, the relative rigidity induced by the prolines hampers ring closure and formation of interheavy-chain disulfide bonds is favored.[7] In IgG4, the motif is CPSC, and intrachain disulfide bonds are formed more easily, resulting in an observable amount of noncovalently linked half-molecules.[8] Usually demonstrated with SDS-PAGE, the amounts of the intrachain isomer reported vary widely,[8−14] which reflects differences in culture systems and/or purification and also technical difficulties.[13] Thus far, no evidence has been found that the intrachain isomer of IgG4 can exchange half-molecules without the need for a reducing environment. This may reflect the limitations in both detection of bispecific IgG4 molecules as well as the uncertainty in the actual amounts of intrachain isomer present. Alternatively,

Received: April 20, 2011
Published: May 31, 2011

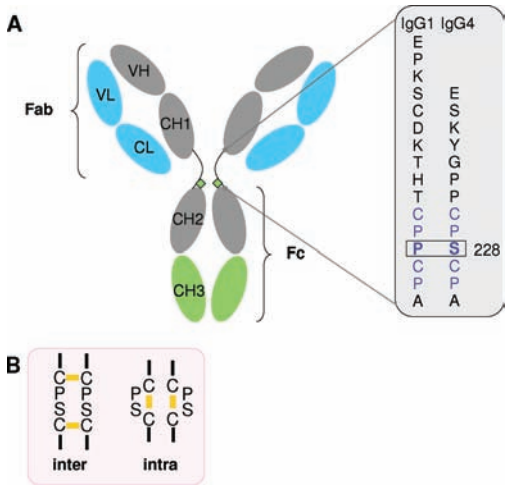

Figure 1. (A) IgG antibody consists of two heavy chains (gray) and two light chains (blue). Between the CH1 and the CH2 domains, a strand of amino acids (hinge region) forms a flexible link between the Fab arms and the Fc arm. Indicated in green are the two features that are important for the exchange reaction of IgG4: the CH3 domain and a serine at position 228. (B) Serine at position 228 in IgG4 introduces flexibility in the core hinge region. Besides the usual disulfide bonds connecting two heavy chains (interchain; indicated in yellow), intrachain disulfide bonds may form instead. In the intrachain isomer the heavy chains are only noncovalently bound.

it has been suggested that the intrachain isomer may be stabilized by additional contacts between CH1 domains in both Fab arms with CH2 domains in the respective neighboring heavy chains,[15] and several studies support this hypothesis.[16,17]

The exchange reaction is expected to proceed by either of two pathways: pathway I, which involves (1) association, (2) reshuffling of disulfide bonds, and (3) dissociation, or pathway II, which involves (1) breaking of interheavy chain disulfide bonds, (2) dissociation, (3) reassociation, and (4) reformation of disulfide bonds. The first mechanism is supported by the fact that association of IgG4 molecules via Fc−Fc interactions was observed,[18] albeit not in the fluid phase. The second mechanism is a likely alternative. However, as mentioned above, the second step (dissociation) is expected to take place for the intrachain isomer spontaneously (i.e., in the absence of a reducing agent), which has not been observed so far.

Here, we present results of a mechanistic study of the IgG4 half-molecule exchange process. The aim of this study was to trace down the individual steps involved in the exchange reaction. Knowledge of its elementary steps may shed light on how this process is controlled in vivo and also contributes to understanding antibody assembly as such. In particular, we wanted to elucidate the role of the hinge region in the exchange reaction and find out if Fab arms indeed play a role in the course of the reaction. In order to do so, we developed two quantitative assays for monitoring the kinetics of the exchange reaction. High-performance size-exclusion chromatography (HP-SEC) was used to separate starting materials and product of the exchange reaction between IgG4 and IgG4 Fc fragments. Moreover, an assay was developed to monitor the reaction in real time and quantitatively using fluorescence spectroscopy. To this end, IgG4 molecules and fragments thereof were tagged with fluorophores that undergo Förster resonance energy transfer (FRET) if only a small distance apart, i.e., if combined into one antibody molecule. This allowed us to unravel the individual steps of the exchange process.

RESULTS

HP-SEC Assay. To monitor the kinetics of the exchange reaction, we first developed an assay where reaction product is separated from starting material based on differences in size. Thus, we incubated IgG4 and IgG4 Fc fragments in the presence of 1 mM GSH as indicated in Figure 2 (this condition was chosen because glutathione is an important biological redox buffer and approximates the in vivo reaction rate obtained from mouse experiments).[2] Samples drawn at different time points and quenched with iodoacetamide were analyzed using HP-SEC. This allows monitoring both the formation of the product as well as the disappearance of starting material. For both, observed kinetics is approximately first order and an observed rate constant of $k_{obs} = 0.14 \times 10^{-3}$ s^{-1} was calculated (Table 1). However, the quenching does not fully prevent the exchange reaction (see Discussion).

FRET Assay. To be able to monitor the exchange process real time without the need for quenching a FRET assay was developed (Figure 3). To this end, IgG4 (natalizumab) was fluorescently labeled with either DyLight488 (Dy488) or DyLight594 (Dy594). This combination of fluorophores was found to be optimal for accurate monitoring of the exchange reaction. To demonstrate the ability for real-time monitoring, both IgG4-Dy488 and IgG4-Dy594 were reduced with dithiothreitol (DTT) and subsequently mixed. A FRET signal appeared in time (Figure 3C), and the resulting kinetics was again first order, yielding a rate constant of $k_{obs} = 2.0 \times 10^{-3}$ s^{-1} (Figure 3D; Table 1). For IgG1, no FRET signal was observed in an analogous experiment. For the exchange reaction with 1 mM of GSH, a rate constant of 0.10×10^{-3} s^{-1} is found in the FRET assay, in close correspondence to the value found in the HP-SEC assay, despite a ca. 100-fold lower concentration of IgG4, see below. The ability to form exchanged product was independently confirmed by using Dy488-anti-*Bet v* 1 IgG4 and Dy594-anti-*Fel d* 1 IgG4, for which bispecific cross-linking activity was observed after incubation at 37 °C with 1 mM GSH (Figure 3B).

Furthermore, hingeless Fc fragments of IgG1 and IgG4, not containing disulfide bonds connecting the heavy chains, were similarly fluorescently labeled. Mixing Dy488 and Dy594-labeled hingeless IgG4 Fc fragments, but not hingeless IgG1 Fc fragments, initiates the exchange process, and formation of mixed product was observed (Figure S2, Supporting Information). A rate constant of $k_{obs} = 1.2 \times 10^{-3}$ s^{-1} was found, close to that found for reduced IgG4 (Table 1). Thus, it appears that by completely reducing all hinge disulfide bonds, the reaction proceeds as if no hinge is present with a rate ca. 20-fold larger than that observed with 1 mM of GSH.

Rate Is Independent of IgG4 Concentration. If association of two IgG4 molecules would be a rate-determining step one would expect the rate to be second order in concentration of IgG4. However, using the HP-SEC assay we found that the observed (first-order) rate constant did not depend on the concentration of Fc (3−12-fold molar excess; Figure 4A). In line with this, for both the exchange reaction of IgG4 at 1 mM of GSH as well as the exchange reaction of IgG4 reduced by DTT, the observed kinetics as monitored with the FRET assay appeared first order and the rate did not depend on the concentration of IgG4 (Figure 4B). It is therefore unlikely that

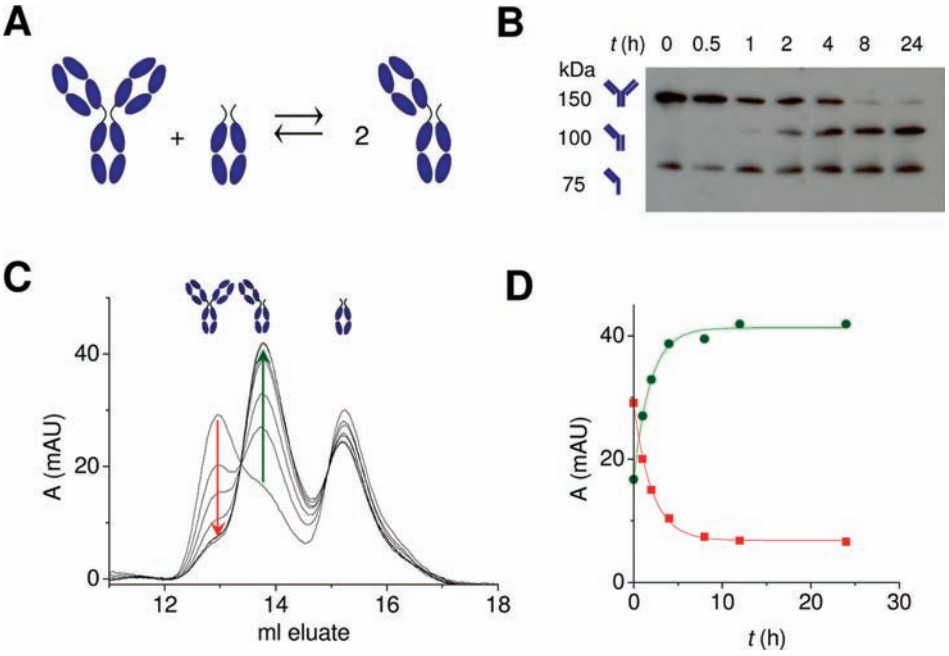

Figure 2. Kinetics of the exchange reaction of IgG4 and IgG4 Fc monitored by HP-SEC and SDS-PAGE. (A) Illustration of the exchange process. IgG4 and IgG4 Fc were incubated (3-fold molar excess of Fc) at 37 °C in the presence of 1 mM GSH, and samples are drawn at different times between 0 and 24 h and quenched by adding iodoacetamide. (B) Nonreducing SDS-PAGE followed by Western blotting (staining for kappa light chain) shows formation of the hybrid 100 kD product, implying that interchain disulfide bonds reform. A similar experiment using silver staining is shown in Figure S1, Supporting Information. (C) Overlay spectrum of HP-SEC runs of the reaction mixture stopped at different time points between 0 and 24 h. (D) Plot of the absorbances indicative of IgG4 (150 kDa; red squares) and the hybrid IgG4/Fc fragment (100 kDa; green dots) vs time. Overall reaction kinetics is close to first order.

Table 1. Observed Rate Constants at 37 °C for the Exchange Reaction of IgG4 or Fragments Thereof

	condition	k_{obs} (10^{-3} s^{-1})
IgG4	reduced	2.0 (0.03)[a,b]
	reduced/alkylated	2.1 (0.1)[b]
	intrachain	1.1 (0.1)[b]
	1 mM GSH	0.10 (0.01)[b]/0.14 (0.02)[c]/0.19 (0.02)[d]
IgG4 Fc	reduced	1.2 (0.05)[b]
	reduced/alkylated	1.6 (0.02)[b]
	intrachain	1.1 (0.1)[b]
	1 mM GSH	0.33 (0.02)[b]/0.47 (0.03)[e]
IgG4 hingeless		1.2 (0.2)[b]

[a] Standard error between parentheses. [b] Value obtained with FRET assay. [c] Value for exchange reaction of IgG4 and IgG4 Fc as determined with HP-SEC assay. [d] Value for exchange reaction of IgG4 and IgG4 CH3 as determined with HP-SEC assay. [e] Value for exchange reaction of IgG4 Fc and IgG4 CH3 as determined with HP-SEC assay.

association of two IgG4 molecules is a rate-determining step. Rather, the perfect first-order kinetics found for both fully reduced IgG4 as well as hingeless IgG4 Fc suggests dissociation into half-molecules to be a likely rate-determining step, at least in case either the hinge is absent or no disulfide bonds in the hinge are present.

Rate Depends on Reduction. The influence of the redox conditions was further examined. The observed rate constant varies with the concentration of GSH but not linearly. Between 0.125 and 5 mM GSH, the observed rate increases from ca. 0.05 to ca. 0.2×10^{-3} s^{-1} as measured in the HP-SEC assay (Figure 4C). This was confirmed using the FRET assay (Figure 4D). Even at 20 mM of GSH, the observed rate is only 0.26×10^{-3} s^{-1}. A slow thiol−disulfide interchange reaction with GSH may underlie this slow rate, since such conversions are reported to sometimes be anomalously slow.[19] On the other hand, reduction of IgG4 is incomplete even with 30 mM of GSH (Figure S4D, Supporting Information), suggesting that GSH induces formation of only a small fraction of noncovalently bound half-molecules, which may cause the low rate constants.

Using the FRET assay a wider range of redox conditions can be reliably studied because quenching of the reaction is not necessary. Thus, with β-mercaptoethanol (BME) a dose dependency is observed between 2 and 20 mM, indicative of a pre-equilibrium rather than a rate-determining reduction step. Indeed, the amount of noncovalently linked IgG half-molecules increases with increasing amounts of BME (Figure S4D, Supporting Information). Again, the observed kinetic profile is close to first order. Using the stronger reducing agent DTT the situation becomes more complicated. If both labeled antibodies are first equilibrated in the presence of DTT, no concentration dependency of the observed rate is found between 0.1 and 3 mM and perfect first-order kinetics is observed. Indeed, hinge disulfide bonds are fully reduced throughout this concentration range (Figure S4A, Supporting Information). Thus, stronger reducing conditions result in faster observed kinetics, with fully reduced IgG4 hitting an upper limit. On the other hand, if the exchange reaction is initiated by adding DTT to the reaction mixture, more complex kinetics is observed, with an initial lag phase followed by near-first-order kinetics (Figure 6B), the latter part being used to

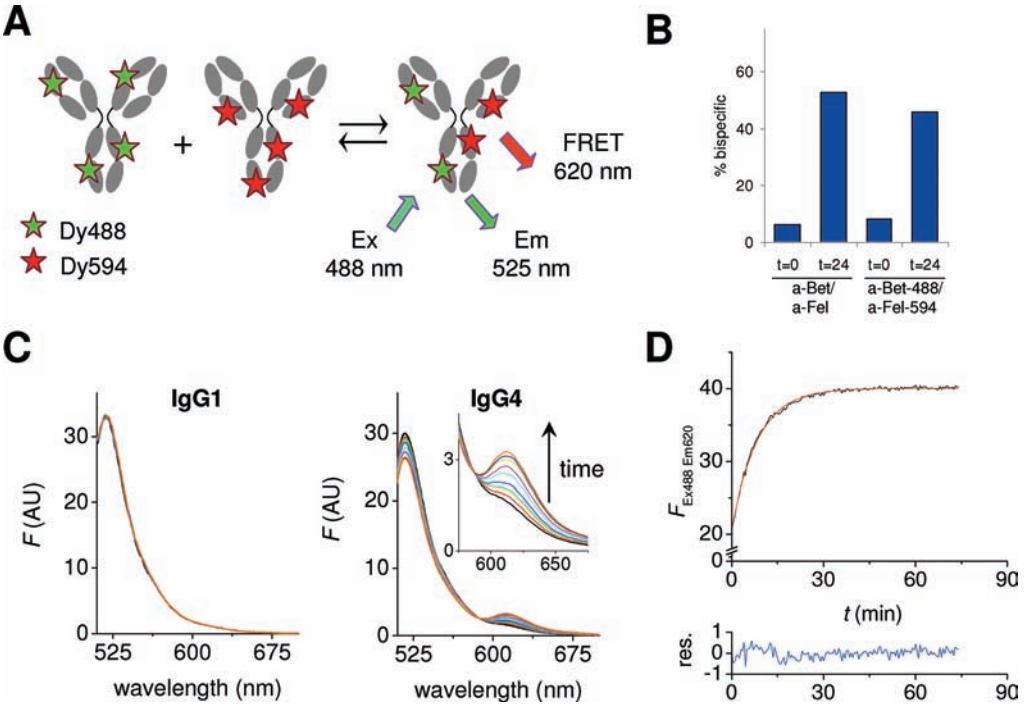

Figure 3. Real-time monitoring of the exchange process using a fluid-phase FRET assay. (A) IgG4 is labeled with either Dy488 or Dy594 fluorochrome, and the reaction is monitored by measuring the FRET signal that arises from the mixed exchange product. (B) Anti-*Bet v* 1 IgG4 was labeled with Dy488 and anti-*Fel d* 1 with Dy594 and incubated (37 °C/1 mM GSH/24 h), and in a cross-linking radioimmunoassay[2] using *Bet v* 1 Sepharose and ^{125}I-labeled *Fel d* 1 it was demonstrated that bispecific antibodies are formed similar to nonlabeled antibodies. (C) Fluorescence overlay spectra of IgG1-Dy488 and IgG1-Dy594 (adalimumab, left panel) or IgG4-Dy488 and IgG4-Dy594 (natalizumab, right panel) mixed and incubated at 37 °C for 60 min after reduction with 1 mM DTT. (D) Rate profile obtained by monitoring the exchange of DTT-reduced IgG4 by measuring the appearance of a FRET signal at 620 nm: (Black curve) experiment; (red curve) fit of a first-order exponential. Lower panel shows residuals of fit.

estimate rate constants that appear in Figure 4D. A more detailed analysis is presented below.

Role Fab Domains. Interestingly, the rates for fully reduced IgG4 and hingeless IgG4 Fc are slightly different (Table 1), suggesting that Fab domains in IgG4 influence the rate. Therefore, the role of the Fab domains on the reaction was further investigated. First, a comparison was made between either IgG4 (I) or IgG4 Fc (II) incubated with CH3 dimers from IgG4 in the presence of 1 mM of GSH (Figure 5A and 5B). The exchange of IgG4 Fc fragments appears to be almost three times faster compared to intact IgG4. However, at $t = 0$, some exchanged product is already visible (most clearly in the case of IgG4/CH3). Quenching with iodoacetamide apparently does not fully prevent the exchange process. Therefore, a similar comparison was made using the FRET assay by incubating fluorescently labeled IgG4 or IgG4 Fc fragments at 1 mM of GSH, and a 3-fold larger rate constant was found for the latter process (Figure 5C). On the other hand, the rate constants for the exchange reactions of both reduced IgG4 Fc and hingeless IgG4 Fc were found to be equal, both being slightly *lower* compared to reduced IgG4 (Figure 5D). As for IgG4, the exchange reactions of either reduced natalizumab or reduced anti-*Fel d* 1 IgG4 proceed at an equal rate (not shown). These results suggest that once the hinge is fully reduced the Fab arms do not contribute to the strength of interaction between the heavy chains. At the same time, the *oxidized* form of the hinge appears to be stabilized by the Fab arms.

Intrachain Isomer. Part of the above-mentioned experiments was carried out using fluorescently labeled natalizumab, a therapeutic IgG4 antibody which was found to contain little of the intrachain isomer.[18] Indeed, in the absence of a reducing agent we did not observe any increase in FRET signal (Figure 5F). On the other hand, using fluorescently labeled anti-*Fel d* 1 IgG4, a small but definite increase in fluorescence was observed in the course of 1 h upon incubating at 37 °C with no reducing agent (Figure 5E). Addition of GSH after 1 h initiated a further exchange reaction. The former process contributes to about 12% of the total increase in fluorescence, which translates to similar amounts of the intrachain isomer being present (Table 2). Thus, by using a sensitive and accurate assay, we are now able to detect a small fraction of intrachain isomers that participates in Fab arm exchange in the absence of any reducing agent. This result implies that isomerization to the intrachain isomer by catalytic action of GSH plays a prominent role in the exchange process at low concentrations of GSH (1 mM and below), because only partial reduction of the hinge disulfide bonds suffices to form this noncovalent isomer, as indicated in Scheme 1. Identical results were obtained if anti-*Fel d* 1 IgG4 was first incubated with 10 mM of oxidized glutathione (GSSG) to force formation of any disulfide bond that might not have formed (not shown), excluding the possibility that part of the hinge disulfide bonds are simply reduced. Using IgG4 Fc fragments, about 17% of the total increase in fluorescence was found if incubated with no reducing agent present (Figure 5F; Table 2).

Kinetic Model of Half-Molecule Exchange. The picture that emerges from all of the above observations is that if no covalent bonds between the heavy chains are present the exchange reaction proceeds via a rate-determining dissociation of the heavy chains. However, for the interchain isomer of IgG4, the interheavy chain disulfide bonds need to be broken for the reaction to take place.

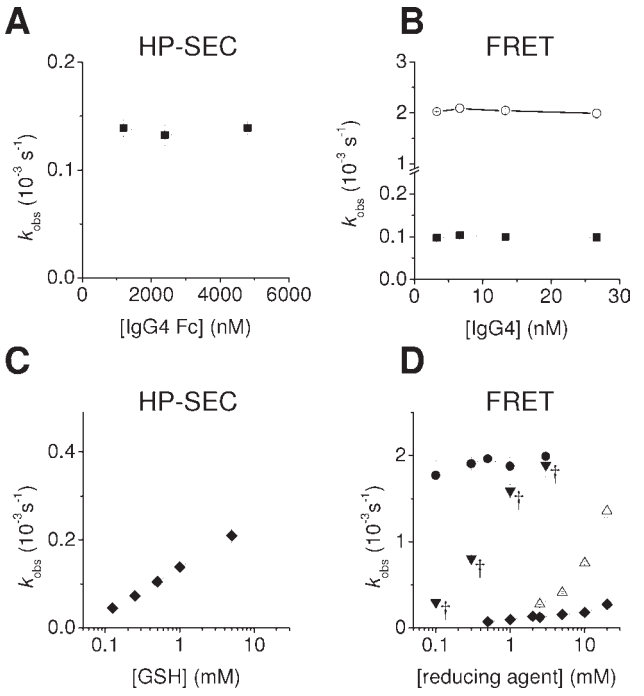

Figure 4. (A) Rate constants for the exchange reaction of IgG4 with different concentrations of IgG4 Fc (3−12-fold excess) at 1 mM of GSH, measured with HP-SEC. (B) Rate constants for the exchange reaction of fluorescently labeled IgG4 (natalizumab) at 1 mM of GSH (■) or after reduction with DTT (○), measured with FRET. (C) Rate constants as in A for different concentrations of GSH. (D) Rate constants as in B for different concentrations of GSH (♦), BME (Δ), and DTT: first reduction then mixing (●) or first mixing then adding DTT (▼). (†) For the latter case, observed rate constants are approximate and do not properly represent the observed kinetics, as shown in Figure 6B.

Below we demonstrate that either the reduction itself becomes rate limiting (in case of DTT) or a pre-equilibrium exists between the interchain and the intrachain isomers, with the overall rate depending on the equilibrium concentration of the latter (in case of GSH).

In order to both qualitatively and quantitatively account for the observed reaction kinetics, we compared the observed kinetics to model predictions for three different cases as illustrated in Figure 6. Details of the derivations and calculations are provided in the Supporting Information. We started with the simplest case, the exchange reaction for hingeless IgG4 Fc fragments (Figure 6A). Initially, an equilibrium between dimers and half-molecules exists for A_2 and A as well as B_2 and B. Upon mixing, heterodimers will form and a new equilibrium will be reached. Differential equations describing this process are shown in Scheme S3, Supporting Information. The observed kinetics, i.e., the FRET signal at 620 nm, is expected to correlate with the appearance of AB and will be reproduced if the dissociation rate is much slower than the association rate and the observed rate constant equals the dissociation rate constant. A value for the dissociation constant (K_d) is required to estimate the individual rate constants. We were able to determine the dissociation constant by monitoring the FRET signal at different concentrations of equimolar amounts of Dy488 and Dy594-labeled hingeless IgG4 Fc (Figure S3 and Table S1, Supporting Information) and assumed the association constant to be equal to $k_a = k_d/K_d$, with k_d being equal to the observed rate constant. Integrating the differential rate equations as detailed in the Supporting Information indeed reproduces the observed kinetics (Figure 6A).

For the second case, the exchange reaction of IgG4 initiated by DTT, a reduction step now precedes the dissociation of half-molecules, as depicted in Figure 6B. Reduction actually proceeds via a number of steps, which is approximated by a single conversion step within the model, described by k_{red} and k_{ox}. Furthermore, we assume that initially only oxidized interchain isomers are present, as is the case for natalizumab. Thus, we estimated rate constants for the reduction of IgG4 (k_{red}) with 0.1 and 0.3 mM of DTT (Figure S4 and Table S2, Supporting Information). We assumed irreversible reduction and therefore arbitrarily assigned a 100-fold lower rate constant to the oxidation reactions. Furthermore, k_d was assumed to equal the rate constant found for reduced IgG4 and k_a was estimated as before. Starting from a mixture of two kinds of oxidized IgG4, integration of the rate equations (Scheme S1, Supporting Information) results in rate profiles that closely match the kinetics observed in case two kinds of (fluorescently labeled) IgG4 are mixed and the exchange reaction started by adding DTT (Figure 6B). Since the reduction rate is comparable or lower than the rate of dissociation, the observed rate profile displays a lag phase, which is reproduced in the simulation. By contrast, if both types of IgG4 antibodies are first reduced and then mixed, the kinetics resembles that of hingeless IgG4 Fc, which is reproduced in a simulation starting from equilibrium values of oxidized (A_2^{OX}, B_2^{OX}), reduced (A_2^{red}, B_2^{red}), and dissociated (A, B) IgG4.

Third, the kinetics of the exchange reactions of IgG4 or IgG4 Fc at 1 mM of GSH was examined. Here, reduction is incomplete, and we expect the most abundant noncovalent isomer to be the intrachain isomer (Discussion), although IgG4 molecules with a (partially) reduced hinge and/or GSH adducts may also be present. The rate of formation of noncovalent isomers was determined (Figure S4 and Table S2, Supporting Information) as well as *equilibrium values for the amounts of noncovalent isomers* (Figure S4F, Supporting Information; Table 2). Using these values and rate constants for the exchange reaction of the intrachain isomers (Table 1) to estimate k_d, rate profiles were calculated (Figure 6C). In this case, the main factor causing the low observed rate of exchange at 1 mM of GSH is the small fraction of intrachain (and/or reduced) isomers present at any time. Compared to the overall reaction rate, a relatively fast pre-equilibrium between covalent and noncovalent isomers precedes the dissociation step, and the faster reaction of IgG4 Fc compared to IgG4 is mainly due to the higher equilibrium value of noncovalent isomers (37% vs 11%, respectively, Table 2). In addition, for natalizumab, starting from very little intrachain isomers, a small lag phase is observed, caused by the finite time it takes before any noncovalent isomers are formed, which subsequently dissociate (inset Figure 6C, Figure S5, Supporting Information).

■ DISCUSSION

Since it was first suggested that IgG4 antibodies are bispecific as a result of half-molecule exchange,[20] the role of the hinge cysteines has remained enigmatic. Although it was recognized that a noncovalent isomer of IgG4 exists without disulfide bonds between the heavy chains, its role in the exchange process could not be determined. In the present study, we were able to unravel the mechanism of the exchange of half-molecules of IgG4 antibodies

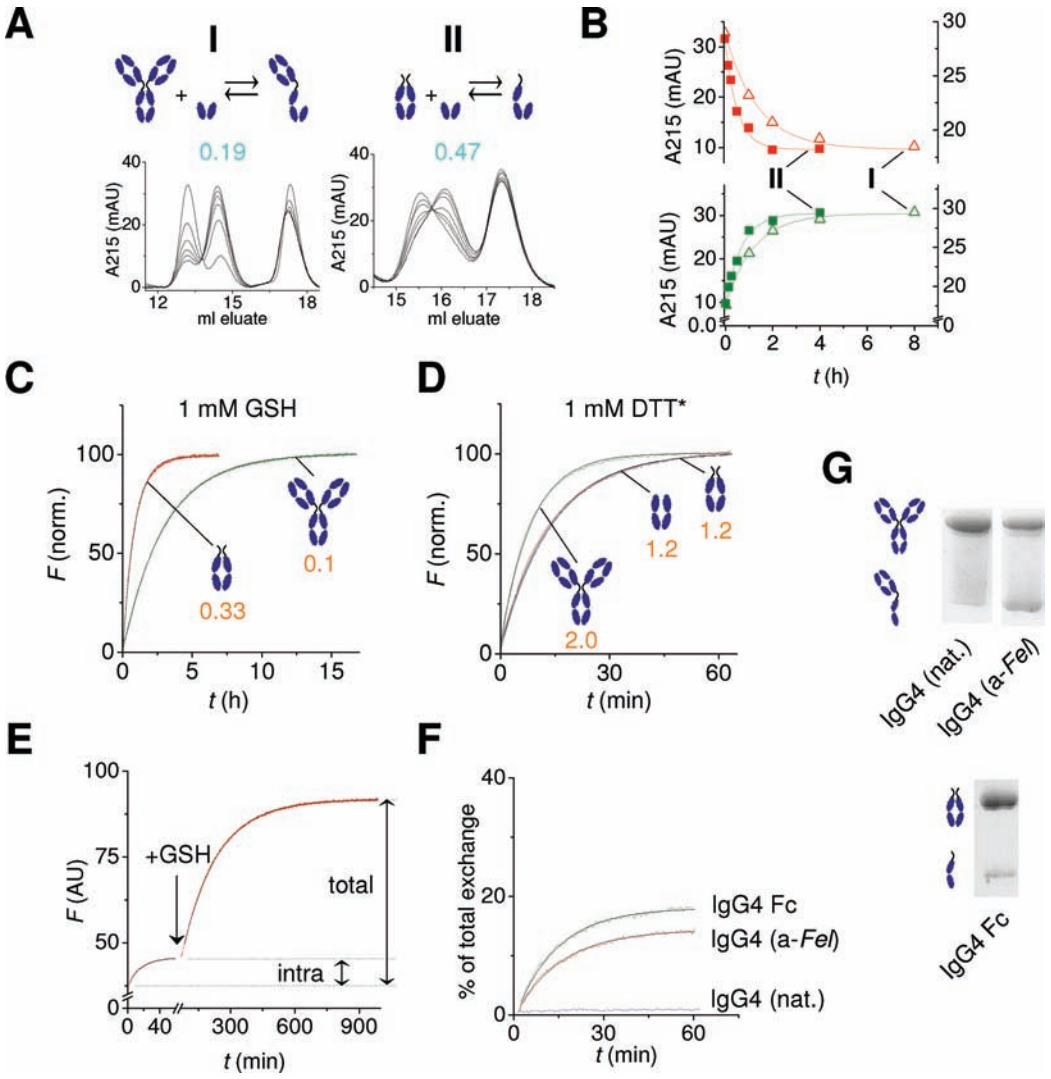

Figure 5. Influence of Fab arms and different isoforms on kinetics. (A) Exchange reaction of either IgG4 or IgG4 Fc with IgG4 CH3 in the presence of 1 mM of GSH as monitored by HP-SEC, also see Figure 2. Compared to IgG4, the reaction of IgG4 Fc with IgG4 CH3 proceeds on average ca. 3-fold faster. Rate constants (10^{-3} s^{-1}) indicated in blue. (B) Appearance of exchange product (green) and disappearance starting material (red) for IgG4 (Δ) or IgG4 Fc (■) as measured in A. Solid lines indicate fits of first-order exponentials to the data. (C) Exchange reaction of IgG4 (natalizumab, green) or IgG4 Fc (red) at 1 mM of GSH as measured in the FRET assay. Black lines indicate fits of first-order exponentials (rate constants indicated in orange, also see Table 1). (D) Exchange reaction of IgG4 (green), IgG4 Fc (red), and hingeless IgG4 Fc (blue) after reduction with 1 mM DTT. Dy488 and Dy594-labeled antibodies or fragments thereof were separately incubated with 1 mM DTT at 37 °C and mixed after 90 min to initiate the reaction. (E) Dy488 and Dy594-labeled IgG4 anti-*Fel d* 1 antibodies were mixed and incubated at 37 °C. A small FRET signal appears in time. After 60 min, GSH was added (1 mM) and a further increase in FRET signal was observed. (F) Exchange reaction of intrachain isomers: natalizumab, anti-*Fel d* 1 IgG4, or IgG4 Fc were incubated in the absence of reducing agent as described in E. For anti-*Fel d* 1 IgG4 and IgG4 Fc, but not for natalizumab, partial exchange was observed. Indeed, for natalizumab, little if any half-molecules were detected using nonreducing SDS-PAGE/Coomassie staining, as shown in G.

by monitoring the kinetics in real time using a sensitive and accurate FRET assay. The level of detail that is provided by this assay resulted in accurate rate profiles displaying subtleties such as an initial lag phase that ultimately lead to a model that adequately describes the kinetics under a variety of conditions. Importantly, we were able to determine rate constants for the exchange reaction of a small portion of intrachain isomers under nonreducing conditions that went previously undetected, probably because the methods used were less sensitive. The results presented in this paper strongly suggest that any noncovalent hinge isomer of IgG4 will participate in Fab-arm exchange, with dissociation of the CH3 domains as the ultimate rate-determining step. At mild reducing conditions the intrachain isomer can form dynamically from the interchain form (Scheme 1), and this equilibrium determines the overall rate.

Fab-arm exchange appears to be much slower in vivo[2] compared to the rate of exchange observed for fully reduced IgG4. This implies that in vivo the process is under control of redox conditions. Blood levels of GSH seem too low to account for the observed exchange reaction.[21] Thus, actual rates of Fab-arm exchange may vary considerably from site to site depending on local redox potentials.

Fab-arm exchange is not limited to endogenous IgG4 but can also take place with therapeutic IgG4 antibodies. Natalizumab is an example of a therapeutic monoclonal antibody based on a wild-type IgG4 that was shown to participate in Fab-arm

Table 2. Amount of Noncovalent Isomers Present in IgG4 and IgG4 Fc

	from vial[a]	1 mM GSH/37 °C[b]
IgG4 natalizumab	<1%	11(2)%[c]
IgG4 anti-*Fel d* 1	12(1)%	n.d.
IgG4 Fc	17(2)%	37(1)%

[a] Estimated as increase in FRET signal with no reducing agent present vs increase in FRET signal in presence of 1 mM GSH. [b] Estimated as an increase in FRET signal after quenching with 10 mM iodoacetamide vs an increase in FRET signal in the presence of 1 mM GSH. [c] Standard error between parentheses.

Scheme 1

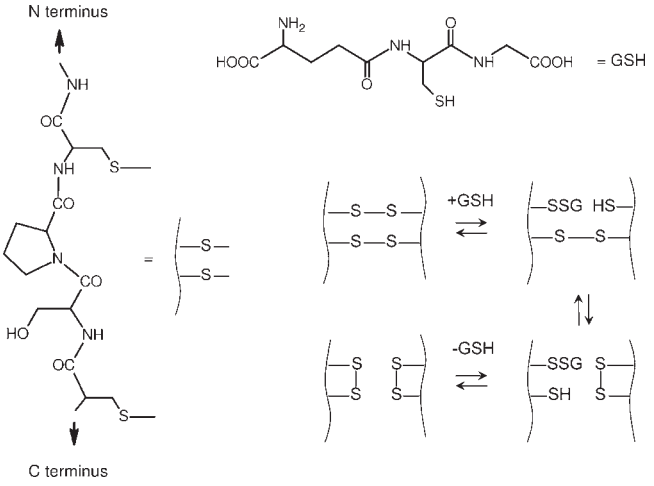

exchange in vivo.[22,23] Most IgG4 therapeutic antibodies in development now possess a hinge with a proline instead of a serine at position 228 in the hinge (as in IgG1, see Figure 1). Such antibodies were shown not to participate in Fab-arm exchange in in vivo animal models.[22,23] However, at higher concentrations of GSH an exchange reaction is observed for these 'hinge-stabilized' IgG4 antibodies.[23] Our preliminary experiments with an hinge-stabilized IgG4 antibody indicate that at 5 mM GSH equilibrium is reached after 2 days, whereas reducing the antibody with DTT results in similar kinetics as wild-type IgG4 (not shown). Thus, Fab-arm exchange may still be observed using 'hinge-stabilized' IgG4 antibodies depending on the redox conditions, and at present it cannot be ruled out that such conditions are never met in vivo. The slow rate of exchange in the presence of GSH probably results from the fact that in contrast to the wild-type hinge, isomerization to the intrachain form is no longer possible. Instead, both disulfide bonds need to be broken before dissociation of half-molecules can take place.

Interestingly, an interplay exists between the Fab arms and the hinge disulfide bonds, such that the Fab arms stabilize the interchain isomer. This may be a unique feature of the CPSC core hinge motif, as opposed to the CPPC motif found in IgG1. In several studies, evidence was found for Fab arms of IgG4 interacting with the CH2 domains in the Fc part,[16,17] which would shield binding sites for C1q and several Fc-gamma receptors. The present data suggest that such an interaction probably is weak. Nevertheless, interaction with most of these receptors is also of intermediate strength,[24] and a shielding of the binding site by Fab arms might thus fine tune these interactions. For human IgG2, another subclass that only weakly triggers effector functions, multiple isomers were described that differ in the connectivity of the hinge isomers,[25] including an intrachain isomer.[26] The structural and functional properties of these hinge isomers warrant further investigation.

Antigen binding may potentially influence the rate of exchange. Previously, we found that fluid-phase IgG4 can bind to IgG4 bound to antigen coupled to a solid support[18] and hypothesized these interactions to represent an intermediate of the exchange reaction. Binding of bivalent IgG4 to antigens on a surface could result in molecular strain that destabilizes the CH3−CH3 interactions in case no disulfide bonds between the heavy chains are present. Therefore, such binding could facilitate dissociation leading to a faster exchange reaction, which would further minimize the cross-linking activity of IgG4.

We found that at mildly reducing conditions, only a modest fraction of IgG4 does not contain covalent bonds between the heavy chains (ca. 12%). This is in contrast to several estimates made using SDS-PAGE by us and others.[9−11] We hypothesize that staining, e.g., using hydrophobic dye may lead to intensities for interchain and intrachain isomers that cannot be directly compared. The relatively small fraction of intrachain isomers is also in line with the results obtained using the HP-SEC assay, in which the reaction was quenched using iodoacetamide, leaving the fraction of intrachain isomers unchanged and able to exchange. Since samples were stored before analysis, this resulted in a systematic deviation that did not influence the analysis of the kinetics.

One may wonder how the strength of interaction of IgG4 CH3 domains (2−4 nM, Table S1, Supporting Information) compares to other antibodies. Stability and dimerization of mouse IgG1 CH3 domains was studied in detail by Buchner et al.[27−29] These studies show that for mouse IgG1 CH3, folding and dimerization are coupled processes. However, since this dimer is very stable, dissociation could be studied only under denaturing conditions. For human IgG1 CH3 an upper bound of 0.1 nM was estimated for the dissociation constant.[30] We monitored the exchange process of hingeless IgG1 fragments for a period of 4 weeks and observed a slow increase in FRET signal. A ca. 5000-fold lower rate constant compared to IgG4 was estimated from these data, which roughly translates to a similarly lower K_d. However, at this stage, we cannot exclude formation of soluble aggregates to be the cause of the observed FRET signal, and further studies are currently being carried out.

In summary, using a sensitive and quantitative real-time FRET assay we obtained accurate kinetic data for the process of half-molecule exchange of human IgG4 antibodies. From the data a reaction mechanism could be deduced involving reduction or isomerization of hinge disulfide bonds followed by a rate-determining dissociation of the heavy chains, which was found to qualitatively and quantitatively account for the observed kinetics based on model calculations. Furthermore, Fab domains were found to influence the course of the reaction. The results imply that in vivo the reaction is under control of redox processes and therefore depends on local redox conditions. We suggest that an experimental approach as described here can be extended to study interdomain interactions also in other antibodies as well as homo-oligomerization by other proteins.

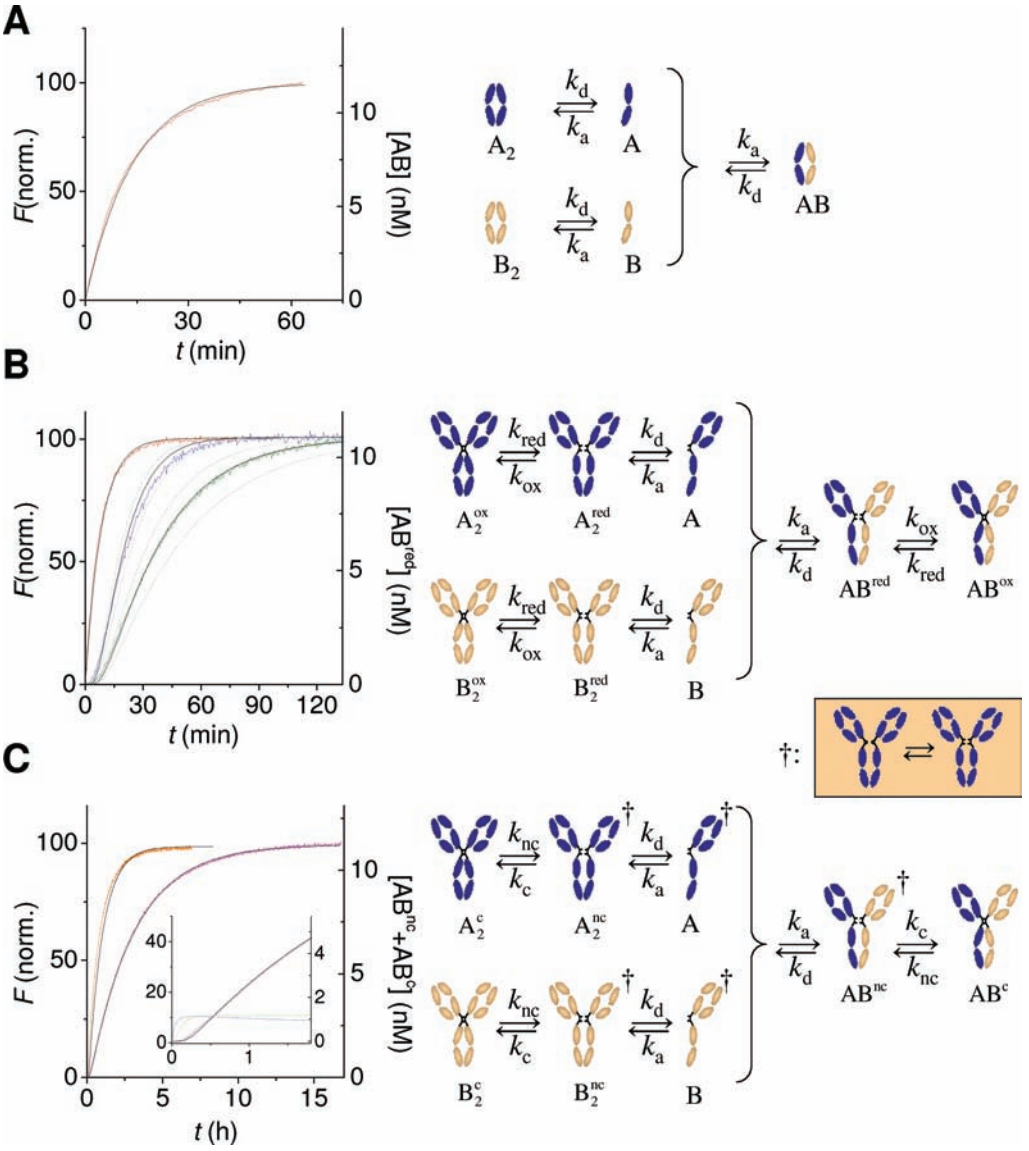

Figure 6. Comparison of simulations of the reaction kinetics (see Supporting Information) with experiment. (A) Exchange reaction of hingeless IgG4 Fc. A_2 is in equilibrium with A, as is B_2 with B. Upon mixing, a new equilibrium is established. The rate profile for formation of exchange product AB is nearly identical to a first-order profile, with a rate constant equal to k_d: (red line) experiment, (black line) simulation. (B) Exchange reaction of IgG4 (natalizumab) with DTT. (I) Starting from IgG4 in the oxidized form, hinge disulfide bonds are reduced by DTT, after which dissociation into half-molecules and formation of exchange product (mainly AB^{red}) will take place. Experimental rate profiles as determined using the FRET assay are shown for 0.1 (green) and 0.3 (blue) mM of DTT, together with simulated rate profiles (black lines). Also shown are simulations for upper and lower estimates of the rates of reduction (dotted gray lines) as listed in Table S2, Supporting Information. (II) By separately reducing two kinds of IgG4, a dynamic equilibrium of reduced IgG4 and half-molecules is established. Assuming near-complete reduction, mixing these results in first-order kinetics: (red line) experiment, (black line) simulation. (C) Exchange reaction of IgG4 (magenta) and IgG4 Fc (orange) with 1 mM GSH. The model is the same as above (Scheme S1, Supporting Information), except that the reduction is incomplete and both reduced IgG4 as well as intrachain isomers are present. For sake of simplicity, we assumed all noncovalent isomers to dissociate at a similar rate k_d. Simulations (black lines) closely resemble experiment. Inset: an initial lag phase is also observed with GSH for natalizumab, which is reproduced by the model, and is caused by the finite time for forming A_2^{nc} and B_2^{nc} (dashed blue line) and A and B (dashed green line) as demonstrated by the simulation.

EXPERIMENTAL SECTION

Materials. Recombinant chimeric IgG1 and IgG4 antibodies against *Fel d 1* and *Bet v 1* were produced as described previously;[2] Fc fragments of IgG1 and IgG4 were obtained as described.[218] Other monoclonal chimeric or human(ized) IgG1 and IgG4 antibodies used are natalizumab (Tysabri, Biogen Idec, Inc.) and adalimumab (Humira, Abbott). IgG4 CH3 fragments were prepared as described in ref 31.

Hingeless Fc fragments of IgG1 and IgG4 were prepared by digestion of 5 mg of adalimumab and natalizumab, respectively, using 1000 U IdeS (Fabricator) protease (Genovis, Sweden). F(ab)2 and hingeless Fc were separated by HP-SEC.

Exchange Reaction: HP-SEC. IgG4 (natalizumab or anti-*Fel d* 1 IgG4) was mixed with IgG4 Fc and incubated with 0.125−5 mM reduced glutathione (GSH; Sigma) in degassed PBS. The final concentration of both IgG4 and IgG4 Fc was 20 μg/mL, unless indicated otherwise. The mixtures were incubated at 37 °C for 24 h, and samples (70 μL) were drawn at various

times between $t = 0$ and 24 h and quenched by adding a 2-fold molar excess of iodoacetamide compared to GSH. Samples were stored at 4 °C until they were analyzed (see below). Reactions of IgG4 with IgG4 CH3 and IgG4 Fc with IgG4 CH3 were carried out analogously.

Size-Exclusion Chromatography. Samples (50 μL) were applied using an autosampler to a Superdex 200 HR 10/30 column (Amersham Biosciences, Uppsala, Sweden), which was connected to a HPLC system (ÄKTAexplorer) from Amersham Biosciences, Uppsala, Sweden. The column was equilibrated in PBS. For estimation of protein size, the column was calibrated with the HMW calibration kit from GE Healthcare. Elution profiles were monitored by measuring UV absorption at 214 nm. For the analysis of overlay spectra, elution profiles were normalized with respect to total peak area to accommodate the variation in recovery that was observed (typically a variation within 15% was found).

SDS-PAGE. Nonreducing SDS-PAGE was performed according to the instructions of the manufacturer (Invitrogen, Carlsbad, CA). Samples were heated for 10 min at 70 °C. Iodoacetamide was added to the sample buffer to minimize artifacts.[32] Gradient gels of 4−12% were used. Gels were stained with Coomassie brilliant blue or silver staining (Invitrogen). Alternatively, for Western blotting, protein was subsequently transferred to nitrocellulose membranes (Invitrogen). Blots were incubated with HRP conjugates of antihuman kappa light chain (Sanquin) and developed with Super Signal West Pico Chemiluminescent substrate (Thermo Scientific).

FRET. IgG and fragments of IgG were labeled with DyLight488 or DyLight594 fluorophore (Pierce/Thermo Scientific). These are amine-reactive dyes that attach to lysine residues. Unreacted dye was removed by repeated dilution/concentration using Amicon Centriprep centrifugal filter devices (Millipore, Billerica, MA) until no dye could be detected anymore in the filtrate. The average degree of labeling (DOF) was between 4 and 6 for IgG1/4 and 2 for IgG1/4 Fc and hingeless IgG1/4 Fc.

Reactions were carried out in quartz cuvettes with an inner chamber volume of ca. 0.25 mL, thermostatted to 37 °C unless indicted otherwise. The reactions were typically carried out using one of the following protocols: (A) 2 μg/mL of IgG4-488 and IgG4-594 in PBS-P (degassed PBS containing 0.05% poloxamer 407 (Lutrol F127, BASF)) were mixed and equilibrated at 37 °C. We found this poloxamer to be an excellent agent for preventing adsorption of IgG to the container walls, in accordance with its potential for preventing microspheres to become opsonized with IgG.[33] Then the reaction was initiated by adding several microliters of a concentrated stock solution of reducing agent (GSH, BME, DTT) to a final concentration of between 0.1 and 20 mM. (B) A 4 μg/mL amount of IgG4-488 and IgG4-594 were incubated separately for 1 h at 37 °C in the presence of reducing agent. Then, the reaction was initiated by mixing equal volumes of both solutions. Kinetics was monitored by measuring the appearance of a FRET signal using a Varian Cary Eclipse fluorescence spectrophotometer equipped with a thermostatted multicell holder (excitation 488 nm, emission 620 nm). To cover the initial kinetics of the faster reactions, dead time was reduced from ca. 100 to ca. 10 s by monitoring a single reaction at a time. To compare experimental rate profiles, normalized fluorescence was calculated as $F(\text{norm.}) = 100 \times (F_t - F_0)/(F_{max} - F_0)$, with F_t being the fluorescence at time t, F_0 fluorescence at $t = 0$, and F_{max} the end-point fluorescence. Overlay plots were determined by recording fluorescence spectra at successive time points after the reaction was started (excitation 488 nm, emission 510−700 nm, 120 nm/min).

Equilibrium Constants. Equilibrium constants were determined by recording fluorescence spectra of 2-fold dilutions of equimolar mixtures of IgG4-Dy488 and IgG4-Dy594, IgG4 Fc Dy488/594, or hingeless IgG4 Fc Dy488/Dy594 in PBS-P after incubation for 2 h at 37 °C. In the case of IgG4 and IgG4 Fc, the buffer also contained 3 mM DTT. Spectra were corrected for background fluorescence, and the ratio of F_{615}/F_{588} was plotted against total concentrations of half-molecules (A + B) to obtain a dose−response curve, F_{588} being the isosbestic point as obtained from kinetic experiments. Since the concentration of mixed IgG4 dimers (AB) will correlate linearly with the total amount of IgG4 dimers ($A_2 + B_2 + AB$), the FRET signal is representative of the amount of dimers present in solution. A 1:1 dimerization model was fitted to the data to determine the dissociation constant.

Isomers without Interheavy Chain Disulfide Bonds. To estimate the amount of intrachain isomers, Dy488 and Dy594-labeled natalizumab, anti-*Fel d* 1 IgG4, or IgG4 Fc were mixed and the reaction kinetics at 37 °C monitored by FRET as described above; after a stable end-point value was reached, GSH was added to a final concentration of 1 mM and the reaction again monitored. The percentage of intrachain isomers was then assumed to equal the percentage of total exchange, calculated as $100 \times (F_{max}^{\text{intrachain}} - F_0)/(F_{max}^{\text{1 mM GSH}} - F_0)$.

The kinetics of formation of isomers without interheavy chain disulfide bonds (i.e., intrachain and reduced isomers) was determined by separately incubating Dy488 and Dy594-labeled natalizumab or IgG4 Fc fragments with either 1 mM GSH or 0.1 or 0.3 mM DTT at 37 °C. Samples were drawn at different time points and quenched by adding iodoacetamide to a final concentration of 10 mM. Then, the exchange reaction was monitored as described above for each time point after mixing both quenched samples. The end-point fluorescence values (taken as F_{620}/F_{588} to account for variations in absolute fluorescence between measurements) were plotted vs time of incubation to obtain the kinetics of formation of isomers without interheavy chain disulfide bonds. Examples are given in Figure S4, Supporting Information. Equilibrium values of the amounts of isomers without interheavy chain disulfide bonds were estimated by comparing the end-point FRET signals from runs in which samples of Dy488 and Dy594-labeled natalizumab (or IgG4 Fc fragments) were mixed after incubation for 120 min with 1 mM of GSH and either quenched or not quenched with iodoacetamide.

Kinetics of Reduction of IgG4 with DTT (SDS-PAGE). Natalizumab was incubated with 0.1, 0.3, 1, or 3 mM of DTT at 37 °C, and samples were drawn at different time points and quenched with iodoacetamide. Samples were analyzed using nonreduced SDS-PAGE as described above. For 0.1 and 0.3 mM, kinetics was quantified by calculating density profiles using ImageJ software. Intensities of bands representing 150 kDa isomers (H_2L_2) were plotted vs time, and an exponential decay was fitted to the data. An example is given in Figure S4, Supporting Information.

Kinetic Modeling. *HP-SEC.* Appearance of the reaction product (100 kD for IgG4/IgG4 Fc; 87 kD for IgG4/IgG4 CH3; 37 kD for IgG4 Fc/IgG4 CH3) or disappearance of the starting material (150 kD for IgG4; 50 kD for IgG4 Fc) was monitored by plotting the peak heights at the respective positions in the elution profiles at various time points. Since overall kinetics appeared to be first order, a single exponential was fitted to the data yielding first-order observed rate constants. The reactions of either natalizumab or anti-*Fel d* 1 IgG4 with IgG4 Fc proceeded at equal rate.

FRET. Appearance of the reaction product was monitored by measuring the increase of FRET signal at 620 nm. Where appropriate, single exponentials were fitted to the data yielding first-order rate constants. Residuals were inspected for the absence of systematic deviations from the fitted model.

Numerical integrations. Model predictions were obtained by numerical integrations of the set of differential equations (Schemes S1 and S3, Supporting Information) using a fourth-order Runge−Kutta algoritm[34] with a fixed step size of 0.6 ms. Detailed description of the model as well as of the parameters used in the calculations can be found in the Supporting Information.

■ ASSOCIATED CONTENT

Supporting Information. Description of the kinetic model (Scheme S1-S3), additional kinetic experiments (Figures S1, S2,

S4, Table S2), determination of dissociation constants (Figure S3, Table S1), and details of the numerical integrations (Figure S5). This material is available free of charge via the Internet at http://pubs.acs.org.

AUTHOR INFORMATION

Corresponding Author
T.Rispens@sanquin.nl

ACKNOWLEDGMENT

The authors thank Sander Meijer for critical reading of the manuscript.

REFERENCES

(1) Liu, H.; Gaza-Bulseco, G.; Faldu, D.; Chumsae, C.; Sun, J. *J. Pharm. Sci.* **2008**, *97* (7), 2426–2447.
(2) van der Neut Kolfschoten., M.; Schuurman, J.; Losen, M.; Bleeker, W. K.; Martinez-Martinez, P.; Vermeulen, E.; den Bleker, T. H.; Wiegman, L.; Vink, T.; Aarden, L. A.; De Baets, M. H.; van de Winkel, J. G.; Aalberse, R. C.; Parren, P. W. *Science* **2007**, *317* (5844), 1554–1557.
(3) Aalberse, R. C.; Stapel, S. O.; Schuurman, J.; Rispens, T. *Clin. Exp. Allergy* **2009**, *39* (4), 469–477.
(4) Wang, W.; Xu, R.; Li, J. *PLoS ONE.* **2010**, *5* (6), e10879.
(5) Lewis, K. B.; Meengs, B.; Bondensgaard, K.; Chin, L.; Hughes, S. D.; Kjaer, B.; Lund, S.; Wang, L. *Mol. Immunol.* **2009**, *46* (16), 3488–3494.
(6) Chivers, P. T.; Prehoda, K. E.; Raines, R. T. *Biochemistry* **1997**, *36* (14), 4061–4066.
(7) Bloom, J. W.; Madanat, M. S.; Marriott, D.; Wong, T.; Chan, S. Y. *Protein Sci.* **1997**, *6* (2), 407–415.
(8) Angal, S.; King, D. J.; Bodmer, M. W.; Turner, A.; Lawson, A. D.; Roberts, G.; Pedley, B.; Adair, J. R. *Mol. Immunol.* **1993**, *30* (1), 105–108.
(9) Schuurman, J.; Perdok, G. J.; Gorter, A. D.; Aalberse, R. C. *Mol. Immunol.* **2001**, *38* (1), 1–8.
(10) Tan, L. K.; Shopes, R. J.; Oi, V. T.; Morrison, S. L. *Proc. Natl. Acad. Sci. U.S.A* **1990**, *87* (1), 162–166.
(11) Norderhaug, L.; Brekke, O. H.; Bremnes, B.; Sandin, R.; Aase, A.; Michaelsen, T. E.; Sandlie, I. *Eur. J. Immunol.* **1991**, *21* (10), 2379–2384.
(12) King, D. J.; Adair, J. R.; Angal, S.; Low, D. C.; Proudfoot, K. A.; Lloyd, J. C.; Bodmer, M. W.; Yarranton, G. T. *Biochem. J.* **1992**, *281* (Pt 2), 317–323.
(13) Taylor, F. R.; Prentice, H. L.; Garber, E. A.; Fajardo, H. A.; Vasilyeva, E.; Blake, P. R. *Anal. Biochem.* **2006**, *353* (2), 204–208.
(14) Forrer, K.; Hammer, S.; Helk, B. *Anal. Biochem.* **2004**, *334* (1), 81–88.
(15) Aalberse, R. C.; Schuurman, J. *Immunology* **2002**, *105* (1), 9–19.
(16) Lu, Y.; Harding, S. E.; Michaelsen, T. E.; Longman, E.; Davis, K. G.; Ortega, A.; Grossmann, J. G.; Sandlie, I.; Garcia, d. l. T. *Biophys. J.* **2007**, *93* (11), 3733–3744.
(17) Abe, Y.; Gor, J.; Bracewell, D. G.; Perkins, S. J.; Dalby, P. A. *Biochem. J.* **2010**, *432* (1), 101–111.
(18) Rispens, T.; Ooievaar-De Heer, P.; Vermeulen, E.; Schuurman, J.; van der Neut Kolfschoten., M.; Aalberse, R. C. *J. Immunol.* **2009**, *182* (7), 4275–4281.
(19) Shaked, Z.; Szajewski, R. P.; Whitesides, G. M. *Biochemistry* **1980**, *19* (18), 4156–4166.
(20) Schuurman, J.; Van, R. R.; Perdok, G. J.; Van Doorn, H. R.; Tan, K. Y.; Aalberse, R. C. *Immunology* **1999**, *97* (4), 693–698.
(21) Jones, D. P.; Liang, Y. *Free Radical Biol. Med.* **2009**, *47* (10), 1329–1338.
(22) Stubenrauch, K.; Wessels, U.; Regula, J. T.; Kettenberger, H.; Schleypen, J.; Kohnert, U. *Drug Metab. Dispos.* **2010**, *38* (1), 84–91.
(23) Labrijn, A. F.; Buijsse, A. O.; van den Bremer, E. T.; Verwilligen, A. Y.; Bleeker, W. K.; Thorpe, S. J.; Killestein, J.; Polman, C. H.; Aalberse, R. C.; Schuurman, J.; van de Winkel, J. G.; Parren, P. W. *Nat. Biotechnol.* **2009**, *27* (8), 767–771.
(24) Bruhns, P.; Iannascoli, B.; England, P.; Mancardi, D. A.; Fernandez, N.; Jorieux, S.; Daeron, M. *Blood* **2009**, *113* (16), 3716–3725.
(25) Dillon, T. M.; Ricci, M. S.; Vezina, C.; Flynn, G. C.; Liu, Y. D.; Rehder, D. S.; Plant, M.; Henkle, B.; Li, Y.; Deechongkit, S.; Varnum, B.; Wypych, J.; Balland, A.; Bondarenko, P. V. *J. Biol. Chem.* **2008**, *283* (23), 16206–16215.
(26) Zhang, B.; Harder, A. G.; Connelly, H. M.; Maheu, L. L.; Cockrill, S. L. *Anal. Chem.* **2010**, *82* (3), 1090–1099.
(27) Buchner, J.; Rudolph, R.; Lilie, H. *J. Mol. Biol.* **2002**, *318*, 829–836.
(28) Thies, M. J. W.; Talamo, F.; Mayer, M.; Bell, S.; Ruoppolo, M.; Marino, G.; Buchner, J. *J. Mol. Biol.* **2002**, *319*, 1267–1277.
(29) Thies, M. J.; Mayer, J.; Augustine, J. G.; Frederick, C. A.; Lilie, H.; Buchner, J. *J. Mol. Biol.* **1999**, *293* (1), 67–79.
(30) Dall'Acqua, W.; Simon, A. L.; Mulkerrin, M. G.; Carter, P. *Biochemistry* **1998**, *37* (26), 9266–9273.
(31) Rispens, T.; Himly, M.; Ooievaar-De, H. P.; den Bleker, T. H.; Aalberse, R. C. *Eur. J. Pharm. Sci.* **2010**, *40* (1), 62–68.
(32) Taylor, F. R.; Prentice, H. L.; Garber, E. A.; Fajardo, H. A.; Vasilyeva, E.; Blake, P. R. *Anal. Biochem.* **2006**, *353* (2), 204–208.
(33) Jackson, J. K.; Springate, C. M.; Hunter, W. L.; Burt, H. M. *Biomaterials* **2000**, *21* (14), 1483–1491.
(34) Press, H. W.; Teukolsky, S. A.; Vetterling, W. T.; Flannery, B. P. *Numerical Recipes in Pascal. The art of scientific computing*, 1st ed.; Cambridge University Press: Cambridge, 1989.